Dalton Transactions

ROYAL SOCIETY OF CHEMISTRY

PAPER

View Article Online
View Journal | View Issue

Cite this: *Dalton Trans.*, 2025, **54**, 2005

Synthesis and exploration of a 1*H*-germol-1-ide/pyridine bidentate ligand†

Chenghuan Liu, * Marc Schmidtmann and Thomas Müller *

Received 8th November 2024,
Accepted 9th December 2024

DOI: 10.1039/d4dt03134b

rsc.li/dalton

The synthesis of an anionic [Ge,N]-bidentate ligand based on the combination of an amidopyridinato group with an anionic germolide ring is reported. The potential of the germolide part of this ligand to switch between η^1-(*via* Ge) and η^5-(*via* C_4Ge) coordination modes makes this ligand an interesting synthetic target. Salt metathesis reactions of the potassium salt of this ligand with $GeCl_2$ dioxane and $SnCl_2$ allow the synthesis of bis-germolyl-substituted germylenes and stannylenes with the tetrel atoms in a distorted square pyramidal coordination environment.

Introduction

Anionic 1*H*-tetrol-1-ides show a versatile structural chemistry, similar to that of isoelectronic phospholes.[1] The coordination environment of the heteroelement E might change from trigonal pyramidal (Fig. 1, [**1**]$^-$) with a localised electron lone pair at the element E to trigonal planar ([**2**]$^-$) with the lone pair delocalised across the five-membered ring. There is compelling computational evidence that for the parent compounds (R = H) the localised, pyramidal structure ([**1**]$^-$) is lower in energy.[2,3] The delocalised, planar isomers ([**2**]$^-$) are favoured when the heterocycle is coordinated to metal ions.[4–9] The important role of the substituents at the heterocycle, in particular of the group R at the element, on this delicate equilibrium was highlighted by our recent report on the structure of the potassium silolide [K(18-c-6)][**5**], which surprisingly shows a planar coordination environment of the silicon even for the separated anion.[10] We wanted to explore whether this structural flexibility of the tetrolides can be utilised to design new ligand systems, [**3**]$^-$ and [**4**]$^-$, in which the anionic heterocycle is attached to an additional donor D, tethered to the heteroelement. We hypothesised, that taking advantage of the flexible number of available electrons and coordination sites of the tetrolide ring, these ligand systems could accommodate different metal ions in variable oxidation states. Here we report on our first attempts to combine a 1*H*-germolide with the 2-amidopyridinato[11–14] scaffold to obtain salts of the bidentate anionic [Ge,N] ligand [**6**]$^-$ and to synthesize homoleptic complexes of this ligand with Ge(II) and Sn(II).

Results and discussion

We synthesized the 1-chloro-1-(pyridine)amido-germole **7** as a suitable precursor for an anionic [Ge,N] chelate ligand through salt metathesis between dichlorogermole and the N-lithiated pyridineamine (Scheme 1). The reductive dechlorination of germole chloride **7** with KC_8 in 1 : 2 molar ratio in the presence of one equivalent of 18-crown-6 ether (18-c-6) at −30 °C in toluene afforded the potassium 1-(pyridine)amido-germolide [K(18-c-6)][**6**] in 50% yield (Scheme 1). Notably, the reduction of chlorogermole **7** in the absence of 18-c-6 yields only mixtures of unidentified products, regardless the reductant used (KC_8, K, Na). Both, chlorogermole **7** (see ESI†) and potassium germolide [K(18-c-6)][**6**] are fully characterized by NMR spec-

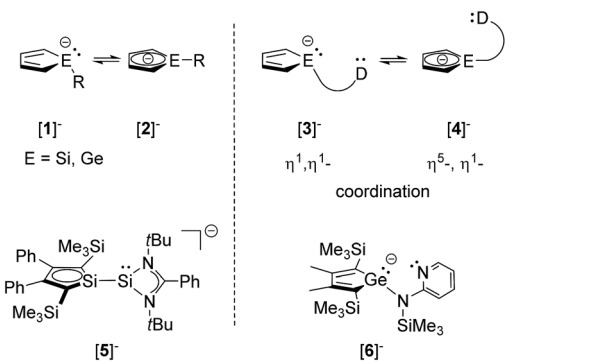

Fig. 1 Possible isomers of 1*H*-tetrol-1-ides ([**1**]$^-$, [**2**]$^-$), of donor-tethered 1*H*-tetrol-1-ides ([**3**]$^-$, [**4**]$^-$), the planar, delocalised silolide [**5**]$^-$ and the targeted germolide [**6**]$^-$.

Institute of Chemistry, Carl von Ossietzky University Oldenburg, Carl von Ossietzky-Str. 9–11, D 26129 Oldenburg, Federal Republic of Germany, European Union.
E-mail: thomas.mueller@uni-oldenburg.de

† Electronic supplementary information (ESI) available. CCDC 2392567–2392570. For ESI and crystallographic data in CIF or other electronic format see DOI: https://doi.org/10.1039/d4dt03134b

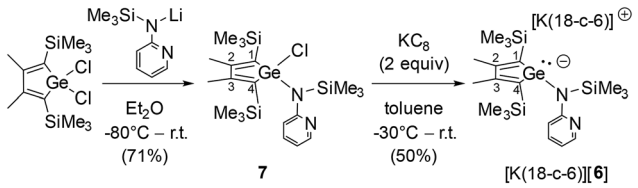

Scheme 1 Synthesis of **7** and [K(18-c-6)][**6**].

troscopy and single crystal X-ray diffraction (sc-XRD) analysis. The complete data is given in the ESI.† The ^{13}C NMR data for the germole ring of [K(18-c-6)][**6**] (δ^{13}C(C$^{1/4}$) = 168.97, δ^{13}C(C$^{2/3}$) = 145.21) are close to those previously reported for the non-planar germole anion in [K(18-c-6)][**9**], but differs significantly from that reported for the anion [**8**]$^-$ with a planar, delocalised germole ring (Scheme 2).[15] This suggests also for potassium germolide [K(18-c-6)][**6**] ion-separation in benzene solution and a germole anion with germanium in a trigonal pyramidal coordination environment.

This is supported by the results of a sc-XRD analysis of air- and moisture sensitive red crystals of [K(18-c-6)][**6**]. The structure solution revealed separated [K(18-c-6)] cation/germolide [**6**]$^-$ ion pairs (Fig. 2). The potassium ion is coordinated to the 18-c-6 and the Ge–K separation is 407.6 pm which is below the sum of the van der Waals radii for both elements (ΣvdW(Ge/K) = 486 pm).[16] It is even larger than those in potassium germolide [K(18-c-6)][**9**] (355.2(4)pm) (Scheme 2).[15] This large Ge/K separation suggests mostly ionic interaction between the isolated potassium cation and germolide anion. The germanium atom adopts a trigonal pyramidal coordination environment with the sum of the bond angles around the germanium atom Ge(1) of Σα(Ge) = 301.3°, which is close to that in [K(18-c-6)][**9**] (Scheme 2). The inner cyclic C/C distances show the typical short-long-short sequence of localised butadienes (C1–C2 137.1, C2–C3 148.4, C3–C4 136.5 pm, Fig. 2) similar to that reported for germolide [**9**]$^-$ (Scheme 2).[15] The amine nitrogen atom N1 takes up a trigonal planar coordination environment and the plane spanned by Si1/N1/C$^\alpha$ bisects the germole ring. The germolide [**6**]$^-$ adopts in the crystal the most stable conformation around the Ge1–N1 and N1–C$^\alpha$ bonds. Notably the conformation [**6a**]$^-$ which is favourable for [Ge,N] chelating coordination is 29 kJ mol^{-1} higher in energy (M06-2X/6-311+G

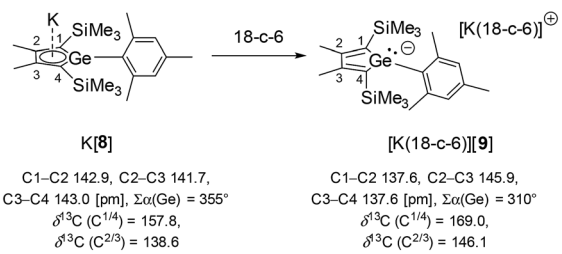

Scheme 2 Isomerisation of germolide [**8**]$^-$ into [**9**]$^-$ triggered by complexation of the potassium counter cation and structural and NMR data pertinent for the discussion.[15]

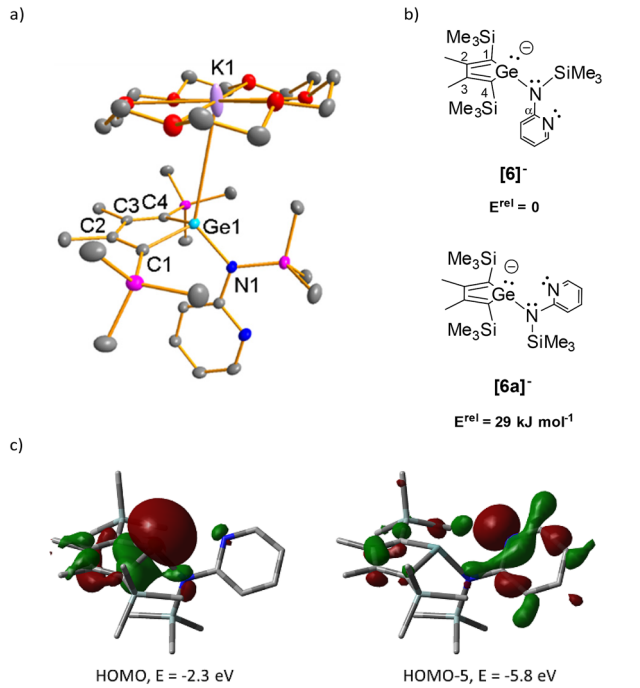

Fig. 2 (a) Molecular structure of the ion pair [K(18-C-6)][**6**] in the crystal. (Hydrogen atoms are omitted for clarity. Thermal ellipsoids are shown at the 50% probability level.) Selected bond lengths [pm] and angles [°]: Ge1–K1 407.6(4), Ge1–C1 198.4(16), Ge1–C4 199.3(14), Ge1–N1 196.4(13), C1–C2 137.1(21), C2–C3 148.4(21), C3–C4 136.5(22), Σα(Ge) 301.3 (sum of the bond angles around Ge1 atom). (b) Relative energies of two conformations of germolide [**6**]$^-$ around the Ge–N and N–C$^\alpha$ bonds, calculated at M06-2X/6-311+G(d,p). (c) Surface diagrams of selected molecular orbitals of germolide [**6a**]$^-$ (M06-2X/6-311+G(d,p), isosurface value: 0.04).

(d,p)).[17] The HOMOs of [**6**]$^-$ and [**6a**]$^-$ are both dominated by a lone pair at the germanium atom with only small contributions of the pyridine nitrogen lone pair, which is however a major contributor to the HOMO−5 (see Fig. 2 for surface diagrams of these MOs of anion [**6a**]$^-$ and ESI† for those of [**6**]$^-$).

We first tested the ability of our new anionic [Ge,N] chelate ligand [**6**]$^-$ to stabilise tetrel elements such as germanium and tin in low oxidation states. For this we treated [K(18-c-6)][**6**] with 0.5 equivalent of GeCl$_2$·dioxane and SnCl$_2$ in Et$_2$O at −30 °C and afforded the stabilised germylene **10** and the stabilised stannylene **11** in good yields (**10**: 31%, **11**: 60%) (Scheme 3). ^{1}H and ^{13}C NMR data along with the results of

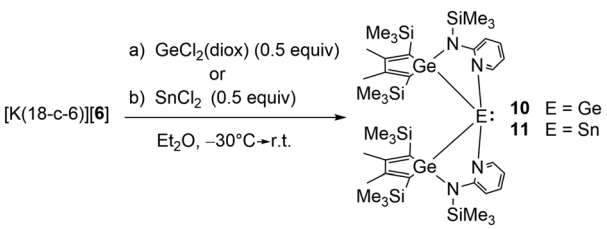

Scheme 3 Synthesis of the stabilised germylene **10** and stannylene **11** (diox: dioxane).

high resolution mass spectrometry confirmed the formation of the product. In addition, stannylene **11** is characterized by a ^{119}Sn NMR resonance signal at δ^{119}Sn = −263.3 which is shifted to significant lower frequencies compared to dicoordinated stannylenes substituted with group 14 elements (*i.e.* stannylenes **12** and **13**, Fig. 3)[18,19] and even compared to pyridine-stabilized stannylenes such as **14** and **15** (Fig. 3).[20,21] This indicates also for stannylene **11** a coordination number of 4 or larger in solution.

The results of sc-XRD analysis confirm for both compounds, **10** and **11**, very similar molecular structures (Fig. 4 and 5). The central tetrel element atoms adopt in both cases a distorted square pyramidal coordination environment. The germanium atoms of the germole rings and the nitrogen atoms of the pyridine substituents span the rectangular basis, and the apical position is occupied by the tetrel element giving space for the remaining lone pair. The Ge–Ge bonds of the stabilized germylene **10** are short single bonds with almost equal lengths of 247 pm (Fig. 4, experimental median value for Ge–Ge: 257–259 pm).[22] The central GeGeGe bond angle of germylene **10** is widened due to the large substituents (α(Ge1Ge2Ge3) = 120.9°). The Ge–N bonds are of different lengths (229 pm, 236 pm) and are significantly larger than the median value for Ge–N single bonds (193.6 pm) but shorter than the sum of the van der Waals radii of the elements germanium and nitrogen (366 pm) and indicate the dative character of the Ge–N interaction.[16,22] The square pyramidal coordination environment and the different Ge–N separations are typical for nitrogen donor stabilised germylenes with the coordination number 4 (*e.g.* germylenes **16**, **17**, Fig. 6),[23–25] although examples with identical Ge–N bonds are reported, for example bis-pyridinyl stabilised germylene **18**.[26]

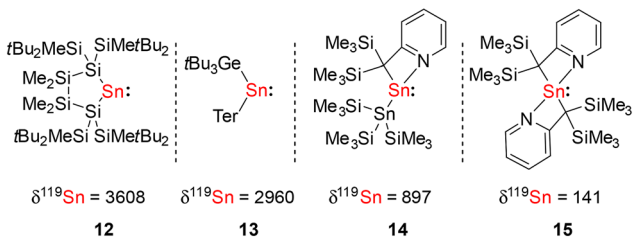

Fig. 3 ^{119}Sn NMR data of selected stannylenes **12–15** pertinent for the discussion (Ter: 2,6-bis-(2,4,6-trimethylphenyl)phenyl).[18–21]

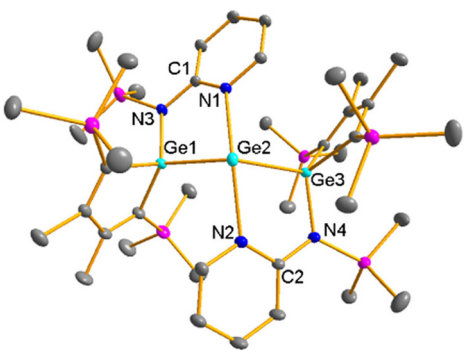

Fig. 4 Molecular structure of germylene **10** in the crystal. (Hydrogen atoms are omitted for clarity. Thermal ellipsoids are shown at the 50% probability level.) Selected bond lengths [pm] and angles [°]: Ge1–Ge2 246.8(4), Ge2–Ge3 246.7(5), N2–Ge2 229.3(9), N1–Ge2 235.8(9), Ge1–Ge2–Ge3 120.9(7), Σα(Ge2) 334.3 (sum of the bond angles around the Ge2 atom).

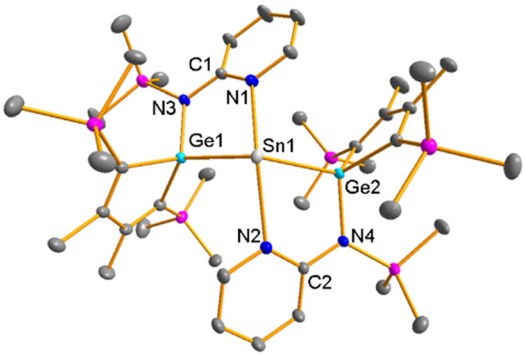

Fig. 5 Molecular structure of **11** in the crystal. (Hydrogen atoms are omitted for clarity. Thermal ellipsoids are shown at the 50% probability level.) Selected bond lengths [pm] and angles [°]: Ge1–Sn1 267.2(4), Ge2–Sn1 266.2(5), N1–Sn1 247.0(6), N2–Sn1 246.9(6), Ge1–Sn1–Ge2 118.0(3), N1–Sn1–N2 144.7(19), Σα(Sn1) 323.6 (sum of the bond angles around the Sn1 atom).

The molecular structure of bis-germylstannylene **11** (Fig. 5) reveals a square pyramidal coordination for the tin atom, close to that of germylene **10**. The Sn–Ge bonds are 267.2 and 266.2 pm in the range of typical Ge–Sn covalent single bond (average/median Ge–Sn: 270 pm).[22] The two Sn/N contacts (247.0, 246.9 pm) are larger than typical Sn–N covalent bonds (Sn–N: 211 pm)[27] but in the typical range reported for pyridinyl-stabilized, tetracoordinated stannylenes (*e.g.* 238–245 pm for stannylene **15**, Fig. 3).[28] The Ge1–Sn1–Ge2 bond angle (118.0°) is larger than in typical dicoordinated stannylenes (90–110°) and is close to that found in NHB_2-Sn (NHB = {B(NDippCH)$_2$}, Dipp = 2,6-i$Pr_2C_6H_3$) reported by Aldridge and coworkers (B–Sn–B = 118.8°).[29]

Bulky substituents in carbene analogues R_2E: (E = Si–Pb) lead to large bond angles at the dicoordinated element E and to a stabilisation of the triplet states relative to their corresponding singlet states. Electropositive substituents like germyl

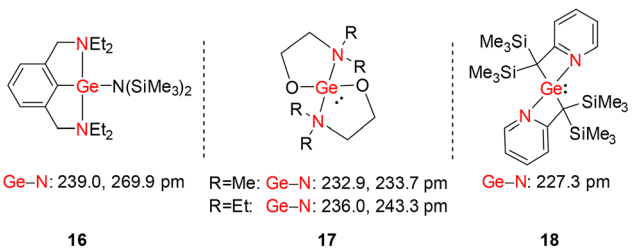

Fig. 6 Structural parameters of selected but typical tetracoordinated germylenes **16–18**.

groups are known to enforce the stabilization of the triplet state.[30–32] For example, DFT computations at the M06-2X/6-311+G(d,p) level predict for bis(trimethylgermyl)germylene $(Me_3Ge)_2Ge$: a rather small vertical singlet–triplet energy gap ΔE_{ST} of 0.53 eV. The results of DFT computations for both bis-germolyl tetrylenes, **10** and **11**, reveal that the singlet states are the ground states, despite their large bond angles. In addition, the calculated ΔE_{ST} are substantial (ΔE_{ST} = 1.58 eV (**10**), 1.54 eV (**11**)). This suggests almost no amphiphilic reactivity of both tetrylenes. Instead, the high energy of the HOMOs (E(HOMO) = −5.9 eV (**10** and **11**)), mainly located at the dicoordinated tetrel element indicates a strong nucleophilic character, typical for these types of stabilized carbene analogues. The bonding situation in both stabilized tetrylenes is very similar and will be discussed only for the germylene **10** in more detail (see ESI†). A natural bond orbital (NBO) analysis[33] reveals two non-polar covalent Ge–Ge bonds, a lone pair, localised at the central germanium atom Ge2 and lone pairs at the pyridine nitrogen atoms that interact with the dicoordinated Ge2 atom (Fig. 7). The calculated Wiberg bond indices (WBIs)[34] for the Ge–Ge bonds (0.92) are typical for Ge–Ge single bonds. The WBIs of the Ge2–N(pyridine) bonds (0.21, 0.23) are significantly smaller than those of the Ge(germolyl)–N(amide) bonds (0.51) in germylene **10** and in amino-substituted germylenes (0.66) and germanes (0.76) (Fig. 8).

The complementary analysis of the computed charge density in the framework of the quantum theory of atoms in molecules (QTAIM)[35] confirms the results of the NBO analysis. The properties of the electron density at the bond critical point (bcp) of germylene **10** classifies the Ge1–Ge2 bond as a shared covalent bond, with all relevant parameters very similar to that of standard compounds (Fig. 9).[36,37] The bonding interaction between the amid nitrogen atom N3 and the germol germanium atom (Ge1) is typified as being strongly polar covalent by the properties of the electron density at the bond critical point (bcp). The bcp is shifted to the electropositive germanium atom and it shows a relative large electron density ρ(bcp), a positive Laplacian $\nabla^2\rho$(bcp) and a negative total energy density H(bcp). Again, the relevant properties of the electron density are very close to those computed for amino substituted germylenes and germanes (Fig. 9). The properties of the bcp for the Ge2/N(pyridine) bond do not differ qualitatively but all values are significantly smaller, which hints to the weaker interaction between these two centres.

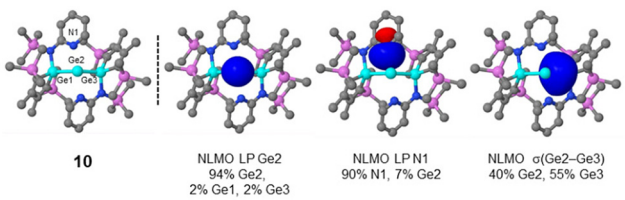

Fig. 7 Computed pertinent NLMOs of **10**, showing the interactions between the dicoordinated germanium atom Ge2 with the germolyl substituents and the remote pyridine ligand (M062X/6-311+G(d,p)), isodensity value 0.04 a.u. (colour code: violet Si, cyan Ge, blue N, gray C).

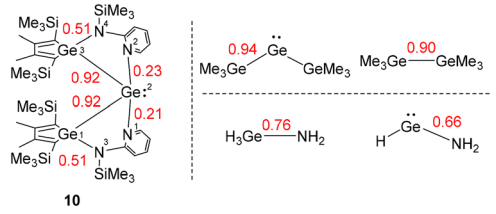

Fig. 8 Computed WBIs (red) of bis-germolyl germylene **10**, and related compounds (M062X/6-311+G(d,p)).

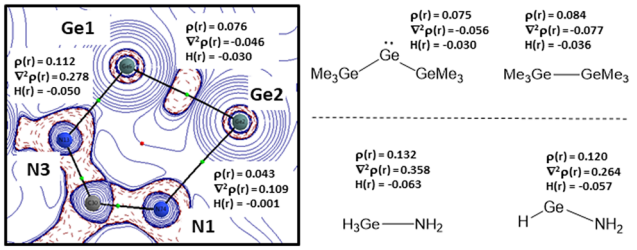

Fig. 9 Results of the QTAIM analysis of bis-germolyl germylene **10**, and related compounds. Left side: part of the molecular graph of germylene **10** projected on a contour plot of the Laplacian of the electron density in the Ge1Ge2N1 plane (green spheres: bond critical points (bcp), red sphere: ring critical point (rcp), electron density at the bcp, $\rho(r)$, in e(Bohr)$^{-3}$; Laplacian at the bcp, $\nabla^2(\rho(r))$, in e(Bohr)$^{-5}$; total energy density at the bcp, $H(r)$, in a.u. (Bohr)$^{-3}$, all calculations at M06-2X/6-311+G(d,p)).

Conclusions

We synthesized a novel bidentate anionic germole/pyridine based ligand $[\mathbf{6}]^-$ starting from a germole dichloride and a 2-aminopyridine. The ligand $[\mathbf{6}]^-$ adopts a localised germole structure and serves as a η^1,η^1-bidentate ligand. This is demonstrated by the salt metathesis reaction with germanium(II) and tin(II) dichloride. The obtained products, the tetracoordinated germylene **10** and stannylene **11**, show a square pyramidal coordination environment of the central atoms. Due to the very similar electronegativity of the Ge atom of the germole substituent and the central element (Ge, **10**, Sn, **11**), the bonds between these centres are regular non-polar covalent bonds, while the interactions between the pyridine-N atom and the central element are strongly polar as expected for coordinative bonds. In general, the bonding situation in both tetracoordinated tetrylenes, **10** and **11**, is as expected for this class of compounds. In particular, even the large bond angles at the central tetrel atom, that are enforced by the bulky germole substituent, do not lead to an appreciable stabilization of the triplet state. For both tetrylenes, singlet triplet energy differences of 1.58 eV and 1.54 eV are calculated, which suggests a predominate nucleophilic reactivity dominated by the high lying HOMO for these carbene analogues.

We are continuing this research and investigate currently the coordination chemistry of the bidentate ligand $[\mathbf{6}]^-$ with transition metal ions.

Author contributions

Investigation, data curation, formal analysis, validation: C. L.; conceptualization, writing, visualization, funding acquisition: C. L., T. M.; project administration, supervision, methodology, resources: T. M.; XRD: M. S.

Data availability

The data supporting this article have been included as part of the ESI.† Original analytical data (source data) are available on request from the corresponding author. Computed molecular structures are given in the ESI† in XYZ coordinates, readable with the CCSD software "Mercury". Crystallographic data for [K(18-C-6)][**6**], **7**, **10** and **11**, has been deposited at the CCDC (2392567–2392570) and can be obtained from [**https://www.ccdc.cam.ac.uk/**].†

Conflicts of interest

There are no conflicts to declare.

Acknowledgements

This work was supported by the Deutsche Forschungsgemeinschaft (DFG) (MU-1440/13-1 and INST 184/227-1). Computations were done at the HPC Cluster CARL, University of Oldenburg, funded by the DFG (INST 184/108-1 FUGG) and the Ministry of Science and Culture (MWK) of the Lower Saxony State. C. L. thanks the China Scholarship Council for support csc no.: 202108330061.

References

1 M. Saito and M. Yoshioka, *Coord. Chem. Rev.*, 2005, **249**, 765–780.
2 J. R. Damewood Jr., *J. Org. Chem.*, 1986, **51**, 5028–5029.
3 B. Goldfuss and P. V. R. Schleyer, *Organometallics*, 1995, **14**, 1553–1555.
4 W. P. Freeman, T. D. Tilley, L. M. Liable-Sands and A. L. Rheingold, *J. Am. Chem. Soc.*, 1996, **118**, 10457–10468.
5 S.-B. Choi and P. Boudjouk, *J. Chem. Soc., Dalton Trans.*, 2000, 841–844.
6 C. Fekete, I. Kovács, L. Nyulászi and T. Holczbauer, *Chem. Commun.*, 2017, **53**, 11064–11067.
7 C. R. W. Reinhold, M. Schmidtmann, B. Tumanskii and T. Müller, *Chem. – Eur. J.*, 2021, **27**, 12063–12068.
8 J. M. Dysard and T. D. Tilley, *J. Am. Chem. Soc.*, 2000, **122**, 3097–3105.
9 W. P. Freeman, J. M. Dysard, T. D. Tilley and A. L. Rheingold, *Organometallics*, 2002, **21**, 1734–1738.
10 C. Liu, M. Schmidtmann and T. Müller, *Chem. Commun.*, 2024, **60**, 11295–11298.
11 R. Kempe, *Eur. J. Inorg. Chem.*, 2003, **2003**, 791–803.
12 D. Jin, A. Hinz, X. Sun and P. W. Roesky, *Chem. – Eur. J.*, 2024, **30**, e202402456.
13 L. Du, H. Wang and Y. Ding, *Polyhedron*, 2017, **134**, 282–286.
14 A. M. Earsad, A. Paparo, M. J. Evans and C. Jones, *Inorganics*, 2024, **12**, DOI: **10.3390/inorganics12100270**.
15 Z. Dong, M. Schmidtmann and T. Müller, *Chem. – Eur. J.*, 2019, **25**, 10858–10865.
16 M. Mantina, A. C. Chamberlin, R. Valero, C. J. Cramer and D. G. Truhlar, *J. Phys. Chem. Sci.*, 2009, **113**, 5806–5812.
17 For computational details, see the ESI.†
18 H. Zhao, J. Li, X.-Q. Xiao, M. Kira, Z. Li and T. Müller, *Chem. – Eur. J.*, 2018, **24**, 5967–5973.
19 W. Setaka, K. Sakamoto, M. Kira and P. P. Power, *Organometallics*, 2001, **20**, 4460–4462.
20 C. J. Cardin, D. J. Cardin, S. P. Constantine, A. K. Todd, S. J. Teat and S. Coles, *Organometallics*, 1998, **17**, 2144–2146.
21 L. M. Engelhardt, B. S. Jolly, M. F. Lappert, C. L. Raston and A. H. White, *J. Chem. Soc., Chem. Commun.*, 1988, 336–338.
22 C. Hemmert and H. Gornitzka, in *Organogermanium Compd.*, 2023, 667–743.
23 C. Bibal, S. Mazières, H. Gornitzka and C. Couret, *Organometallics*, 2002, **21**, 2940–2943.
24 N. N. Zemlyansky, I. V. Borisova, M. G. Kuznetsova, V. N. Khrustalev, Y. A. Ustynyuk, M. S. Nechaev, V. V. Lunin, J. Barrau and G. Rima, *Organometallics*, 2003, **22**, 1675–1681.
25 M. Rusek, G. Bendt, C. Wölper, D. Bläser and S. Schulz, *Z. Anorg. Allg. Chem.*, 2017, **643**, 676–682.
26 G. Ossig, A. Meller, C. Brönneke, O. Müller, M. Schäfer and R. Herbst-Irmer, *Organometallics*, 1997, **16**, 2116–2120.
27 P. Pyykkö and M. Atsumi, *Chem. – Eur. J.*, 2009, **15**, 12770–12779.
28 K. W. Klinkhammer, in *The chemistry of Organic germanium, tin and lead compounds*, ed. Z. Rappoport, John Wiley & Sons, Chichester, 2002, vol. 2, p. 283.
29 A. V. Protchenko, K. H. Birjkumar, D. Dange, A. D. Schwarz, D. Vidovic, C. Jones, N. Kaltsoyannis, P. Mountford and S. Aldridge, *J. Am. Chem. Soc.*, 2012, **134**, 6500–6503.
30 M. S. Gordon and M. W. Schmidt, *Chem. Phys. Lett.*, 1986, **132**, 294–298.
31 R. S. Grev, H. F. Schaefer III and P. P. Gaspar, *J. Am. Chem. Soc.*, 1991, **113**, 5638–5643.
32 M. C. Holthausen, W. Koch and Y. Apeloig, *J. Am. Chem. Soc.*, 1999, **121**, 2623–2624.
33 A. E. Reed, L. A. Curtiss and F. Weinhold, *Chem. Rev.*, 1988, **88**, 899–926.
34 K. B. Wiberg, *Tetrahedron*, 1968, **24**, 1083–1096.

35 R. F. W. Bader, *Atoms in Molecules: A Quantum Theory*, Clarendon, Oxford, 1990.
36 P. Macchi and A. Sironi, *Coord. Chem. Rev.*, 2003, **238–239**, 383–412.
37 J. I. Schweizer, M. G. Scheibel, M. Diefenbach, F. Neumeyer, C. Würtele, N. Kulminskaya, R. Linser, N. Auner, S. Schneider and M. C. Holthausen, *Angew. Chem., Int. Ed.*, 2016, **55**, 1782–1786.